MOLECULAR AND CELLULAR BIOLOGY, Nov. 1997, p. 6339–6347 Vol. 17, No. 11
0270-7306/97/$04.00+0

A Homolog of Mammalian, Voltage-Gated Calcium Channels Mediates Yeast Pheromone-Stimulated Ca^{2+} Uptake and Exacerbates the *cdc1*(Ts) Growth Defect

MADAN PAIDHUNGAT AND STEPHEN GARRETT*

Departments of Molecular Cancer Biology and Biochemistry, Duke University Medical Center, Durham, North Carolina 27710

Received 29 May 1997/Returned for modification 29 July 1997/Accepted 8 August 1997

Previous studies attributed the yeast (*Saccharomyces cerevisiae*) *cdc1*(Ts) growth defect to loss of an Mn^{2+}-dependent function. In this report we show that *cdc1*(Ts) temperature-sensitive growth is also associated with an increase in cytosolic Ca^{2+}. We identified two recessive suppressors of the *cdc1*(Ts) temperature-sensitive growth which block Ca^{2+} uptake and accumulation, suggesting that cytosolic Ca^{2+} exacerbates or is responsible for the *cdc1*(Ts) growth defect. One of the *cdc1*(Ts) suppressors is identical to a gene, *MID1*, recently implicated in mating pheromone-stimulated Ca^{2+} uptake. The gene (*CCH1*) corresponding to the second suppressor encodes a protein that bears significant sequence similarity to the pore-forming subunit (α1) of plasma membrane, voltage-gated Ca^{2+} channels from higher eukaryotes. Strains lacking Mid1 or Cch1 protein exhibit a defect in pheromone-induced Ca^{2+} uptake and consequently lose viability upon mating arrest. The *mid1*Δ and *cch1*Δ mutants also display reduced tolerance to monovalent cations such as Li^+, suggesting a role for Ca^{2+} uptake in the calcineurin-dependent ion stress response. Finally, *mid1*Δ *cch1*Δ double mutants are, by both physiological and genetic criteria, identical to single mutants. These and other results suggest Mid1 and Cch1 are components of a yeast Ca^{2+} channel that may mediate Ca^{2+} uptake in response to mating pheromone, salt stress, and Mn^{2+} depletion.

In eukaryotic cells, cytosolic Ca^{2+} concentration ($[Ca^{2+}]_i$) fluctuates transiently to regulate such diverse processes as neurotransmitter release, muscle contraction, and T-cell activation (9, 31). Intracellular Ca^{2+} levels are tightly regulated by numerous channels, pumps, and antiporters, such that $[Ca^{2+}]_i$ is normally maintained at an extremely low concentration (~ 100 nM) despite a 10,000-fold concentration difference across the plasma membrane (9). Eukaryotic cells utilize this gradient to generate Ca^{2+} spikes by stimulating the opening of Ca^{2+} channels and allowing Ca^{2+} influx down the concentration gradient (9, 31). Among the best characterized of these entry pathways are the voltage-dependent Ca^{2+} channels of the plasma membrane which open in response to membrane depolarization (3, 9).

Ca^{2+} has been implicated in numerous processes of the budding yeast *Saccharomyces cerevisiae* (8, 16, 20, 37), including stress-induced expression of ion transporter genes, bud formation, and viability upon pheromone-induced arrest. However, there is compelling evidence for a role for Ca^{2+} in only the last of these processes (7, 15, 16, 22). Haploid yeast cells exist as two mating types, **a** and α, that secrete mating pheromones **a**- and α-factor, respectively. In the presence of α-factor, **a** cells undergo a complex developmental process in preparation for mating. For example, pheromone-treated cells accumulate high levels of intracellular Ca^{2+}, arrest in G_1, and form a mating projection or shmoo (16). Cells arrested in medium lacking Ca^{2+} lose viability within 5 h after pheromone treatment, and the loss of viability is accompanied by a small-shmoo morphology, suggesting that Ca^{2+} influx is essential for recovery (16). Consistent with this idea, mutants lacking Ca^{2+} response activities of the Ca^{2+}/calmodulin-dependent protein kinase and protein phosphatase (calcineurin) lose viability upon pheromone treatment even in Ca^{2+}-containing medium (7, 22, 35).

An intriguing aspect of the pheromone-induced Ca^{2+} response is the mechanism by which mating factor treatment elicits the influx of Ca^{2+}. Although recognizable Ca^{2+} channels have not been cloned from yeast (4, 13, 27), the *MID1* gene encodes a plasma membrane protein that is required for pheromone-induced Ca^{2+} uptake and viability upon pheromone arrest (15).

We have been studying the physiological role of the essential yeast gene *CDC1*. Neither the biochemical activity nor the physiological function of the *CDC1* product is known; however, recent studies suggest that Cdc1 regulates intracellular Mn^{2+} (20, 25, 32). That conclusion is consistent with the observation that the conditional *cdc1*(Ts) growth defect can be ameliorated by Mn^{2+} supplementation (20, 25). This report shows that *cdc1*(Ts) growth arrest is accompanied by an increase in $[Ca^{2+}]_i$. The increase in cytosolic Ca^{2+} exacerbates the growth defect because two recessive suppressors (*cos10* and *cos2*) of *cdc1*(Ts) conditional growth reduce Ca^{2+} accumulation in wild-type and *cdc1*(Ts) strains. *COS10* is identical to *MID1*, and *COS2* identifies a structural homolog of the large subunit of voltage-dependent Ca^{2+} channels of higher eukaryotes. Both genes are essential for pheromone-stimulated Ca^{2+} influx and affect $[Ca^{2+}]_i$ uptake and accumulation in both *cdc1*(Ts) and wild-type cells. These and other results suggest that the increase in $[Ca^{2+}]_i$ contributes to the *cdc1*(Ts) growth defect and that yeast cells, like their mammalian counterparts, contain channels which allow regulated Ca^{2+} uptake.

MATERIALS AND METHODS

Strains and plasmids. Except where noted, all *S. cerevisiae* strains were derived, by reversion or transformation, from FY11 (*MAT***a** *ade1 trp1 leu2 his3 ura3*

* Corresponding author. Present address: Department of Microbiology and Molecular Genetics, UMDNJ-New Jersey Medical School, 185 South Orange Ave., University Heights, Newark, NJ 07103-2714. Phone: (973) 972-0698. Fax: (973) 972-3644.

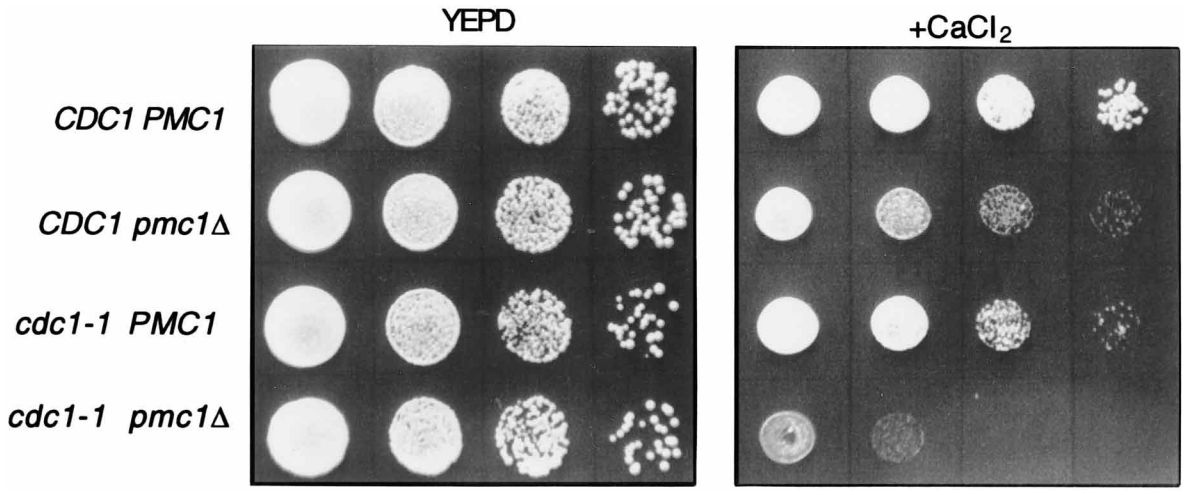

FIG. 1. Ca^{2+} sensitivity of *cdc1*(Ts) and *pmc1*Δ mutants. Tenfold serial dilutions of log-phase cultures of *CDC1 PMC1* ((FY70), *CDC1 pmc1*Δ (FY527), *cdc1-1 PMC1* (FY11), and *cdc1-1 pmc1*Δ (FY526) were spotted onto rich medium agar without (YEPD) or with (+$CaCl_2$) 200 mM $CaCl_2$ and incubated at 23°C for 4 days.

cdc1-1) or its isogenic derivative FY70 (*MAT***a** *ade1 trp1 leu2 his3 ura3 CDC1*). Derivatives of FY388 (*MAT***a** *ade1 trp1 leu2 his3 ura3 cdc1-2*) were obtained by transformation. Bacterial strains MC1066 [*Δ(lac)X74 galU galK strA hsdR trpC9830 leuB6 pyrF*::Tn5] and DH5α {F′/*endA hsdR17*(r^- m^-) *supE44 thi-1 recA1 gyrA relA1* Δ(*lacZYA-argF′)U169* [ϕ80d*lac*Δ*(lacZ)M15*)]} were used for plasmid manipulations and have been described previously (2, 36).

Plasmids carrying *lacZ* fused to *PMC1* (pKC190) and *PMR2A* (pKC201) have been described elsewhere (6), as has the *pmc1*Δ::*LEU2* plasmid (pKC52) used to disrupt *PMC1* (5). Plasmid pCBL contains the *cnb1*Δ::*LEU2* deletion and was obtained from J. Heitman, Duke University Medical Center. Plasmid pJM1485 contains a *JNM1-lacZ* fusion and was obtained from J. McMillan, Duke University Medical Center. The low-copy-number *MID1* plasmid (pFB444) was constructed by inserting a 4.4-kb *Eco*RV fragment containing *MID1* into the *Sma*I site of the *URA3* cloning vector pRS316 (28). The *mid1*Δ::*LEU2* disruption plasmid (pFB457) was constructed in several steps. The 4.4-kb *Eco*RV fragment containing *MID1* was inserted into the *Pvu*II site of the vector pBSIIKS (Stratagene) to create plasmid pFB448. A *Spe*I site was placed in the *MID1* coding region by inserting the small *Eco*RI-*Pst*I fragment from Yep24 (bp 1996 to 2241) into the *Eco*RI-*Pst*I sites of pFB448 to create plasmid pFB449. Finally, a 2.2-kb *Spe*I-*Pst*I fragment containing *LEU2* was inserted into the *Spe*I-*Pst*I sites of pFB449 to create plasmid pFB457. This was necessary to ensure that the *LEU2* insertion did not affect the function of the adjacent gene, *RFC3* (15).

The *cch1*Δ::*LEU2* and *cch1*Δ::*HIS3* disruption plasmids were constructed in two steps. First, a 2.2-kb internal fragment (bp 2218 to 4465 of the coding region) of *CCH1* (obtained by PCR amplification of chromosomal DNA) was inserted into the *Eco*RV site of plasmid pBSIIKS to create plasmid pFB515. The *cch1-1*Δ::*LEU2* and *cch1-2*Δ::*LEU2* plasmids (pFB522 and pFB523, respectively) were constructed from pFB515 by replacing the 1.25-kb *Eco*RV internal fragment of *CCH1* (see Fig. 2) with the 2.2-kb *Hpa*I fragment of *LEU2* in the opposite orientation. The *cch1*Δ::*HIS3* plasmid (pFB538) was constructed from pFB515 by replacing the 1.25-kb *Eco*RV internal fragment of *CCH1* (see Fig. 2) with a *Bgl*II linker and then inserting the 1.7-kb *Bam*HI fragment of *HIS3* into the *Bgl*II site. Because plasmids containing the full-length *CCH1* gene could not be propagated in bacteria, a low-copy-number *CCH1* plasmid was generated by cotransforming a yeast strain with *CCH1* DNA (obtained by PCR) and a yeast vector containing the 5′ and 3′ ends of *CCH1*. A low-copy number plasmid yeast vector containing the 5′ and 3′ ends of *CCH1* (*cch1*Δ::*Hin*dIII, pFB535) was created in several steps. The 5′ end of *CCH1* (bp −993 to 223) was obtained by PCR, digested with *Cla*I (−903) and *Hin*dIII (138), and then ligated into the same sites of pBSIIKS to generate pFB526. The 3′ end of *CCH1* (bp 5319 to 6218) was obtained by PCR and then ligated into the *Eco*RV site of pBSIIKS. A plasmid with the insert oriented correctly (pFB529) was digested with *Hin*dIII (5381) and *Spe*I (multiple cloning site), and the 840-bp 3′ *CCH1* fragment was inserted into the *Hin*dIII and *Spe*I sites of plasmid pFB526 to create pFB533. Finally, the *cch1*Δ::*Hin*dIII fragment was transferred as a *Pvu*II fragment from pFB533 into the *Pvu*II sites of the low-copy-number *URA3* vector pRS316 to obtain pFB535. A 7.3-kb DNA fragment containing the full-length *CCH1* gene (bp −993 to 6218) was amplified from genomic DNA by PCR, using Ex-Taq polymerase from Ta-ka-ra.

Growth media and conditions. Standard yeast media were prepared as previously described (17). α-Factor halo assays were done by adding synthetic pheromone (Sigma) to sterile filter discs placed on a lawn of the appropriate strain (22).

Calcium accumulation and uptake. Calcium accumulation, exchange, and uptake assays used $^{45}Ca^{2+}$ from NEN-Dupont and were done according to published procedures (5, 15) except that for the calcium accumulation assays, 1 μCi of $^{45}Ca^{2+}$ per ml was used.

β-Galactosidase assays. β-Galactosidase activity was measured according to a published procedure (17). Units/0.1 OD_{600} (optical density at 600 nm) were calculated as $(1.7 \times OD_{420})/(0.0045 \times \text{time} \times 0.1\ OD_{600})$.

RESULTS

***cdc1-1*(Ts) mutants are Ca^{2+} sensitive and display an increase in intracellular Ca^{2+}.** During studies of the essential yeast gene *CDC1*, we noticed that two [*cdc1-1*(Ts) and *cdc1-6*(Ts)] of four conditional *cdc1*(Ts) mutants grew slowly at the permissive temperature and were sensitive to high-Ca^{2+} (200 mM) conditions (Fig. 1 and data not shown). A subset of existing Ca^{2+}-sensitive mutants display elevated levels of intracellular Ca^{2+} even in standard, low-Ca^{2+} (200 to 800 μM) media (1, 24, 33). Thus, we examined the Ca^{2+} content of the *cdc1-1*(Ts) mutant by measuring $^{45}Ca^{2+}$ accumulation. At 23°C in YEPD (about 200 μM Ca^{2+}), the *cdc1-1*(Ts) mutant accumulated twice as much intracellular Ca^{2+} as the isogenic *CDC1* strain (Fig. 2). This difference was greater at the nonpermissive temperature, where the *cdc1-1*(Ts) strain accumulated almost seven times as much intracellular Ca^{2+} as the wild-type strain (Fig. 2). Thus, Cdc1 depletion causes cells to hyperaccumulate Ca^{2+}.

The vacuole serves as the major Ca^{2+} store in yeast, and vacuolar Ca^{2+} accumulation is largely dependent on the vacuolar Ca^{2+}-ATPase, Pmc1 (5). Not surprisingly, the Ca^{2+} content of the *cdc1-1*(Ts) *pmc1*Δ strain was only 10 to 20% that of the *cdc1-1*(Ts) mutant, indicating that much of the excess Ca^{2+} was in the vacuole (Fig. 3). Nevertheless, the *cdc1-1*(Ts) *pmc1*Δ mutant accumulated more than twice as much Ca^{2+} as the *CDC1 pmc1*Δ strain (Fig. 3). Thus, the *cdc1-1*(Ts) strain accumulated excess Ca^{2+} in both Pmc1-dependent and Pmc1-independent pools. Most intracellular Ca^{2+} is localized in the vacuole as a nonexchangeable complex with polyphosphate (11). Exchangeable Ca^{2+}, by contrast, is thought to reflect Ca^{2+} pools of the cytoplasm and secretory organelles such as the Golgi (6, 11). Both nonexchangeable (*CDC1*, 562.9 ± 42.6 pmol/OD_{600}; *cdc1-1*, 1,193.5 ± 55.8 pmol/OD_{600}) and exchangeable (*CDC1*, 24.0 ± 18.0 pmol/OD_{600}; *cdc1-1*, 138.3 ± 95.0 pmol/OD_{600}) intracellular pools were altered in the *cdc1-*

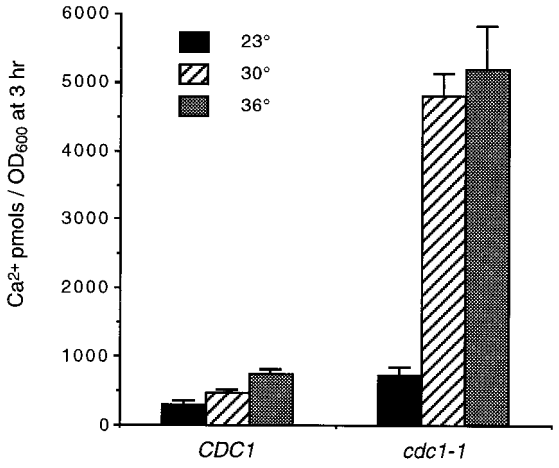

FIG. 2. *CDC1* and Ca^{2+} accumulation. Log-phase cultures were labeled for 3 h at the indicated temperatures in medium containing $^{45}Ca^{2+}$ (1 μCi/ml). Values shown are from one experiment and are representative of results obtained in three independent experiments. Strains were *CDC1* (FY70) and *cdc1-1* (FY11).

1(Ts) mutant. (Exchangeable pools were calculated, as described elsewhere [6, 11], by subtracting the nonexchangeable pools from the total pools. Accordingly, the standard deviations of the exchangeable pools seem high.) Together, these results suggest that *cdc1*(Ts) mutants accumulate Ca^{2+} in the vacuole, as well as in one or more nonvacuolar compartments.

Ca^{2+}/calcineurin-dependent transcription is elevated in *cdc1*(Ts) mutants. Mutations in *PMC1* block vacuolar Ca^{2+} sequestration (Fig. 3; reference 5) and, presumably as a result of the corresponding increase in $[Ca^{2+}]_i$, confer sensitivity to growth on high-Ca^{2+} medium (Fig. 1; reference 5). Deletion of *PMC1* did not alleviate *cdc1-1*(Ts) temperature-sensitive growth (data not shown), suggesting that vacuolar Ca^{2+} accumulation was unrelated to the conditional growth defect. However, *pmc1*Δ did exacerbate *cdc1-1*(Ts) Ca^{2+} sensitivity (Fig. 1), consistent with the notion that $[Ca^{2+}]_i$ is elevated in the

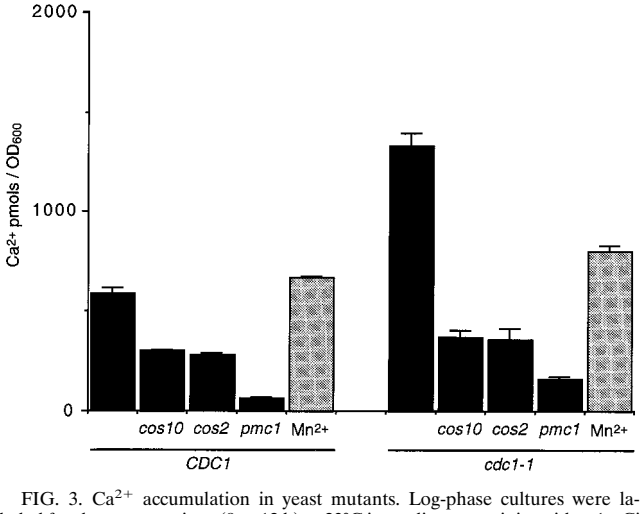

FIG. 3. Ca^{2+} accumulation in yeast mutants. Log-phase cultures were labeled for three generations (9 to 12 h) at 23°C in medium containing either 1 μCi of $^{45}Ca^{2+}$ per ml or 1 μCi of $^{45}Ca^{2+}$ per ml plus 0.5 mM $MnCl_2$. Each value represents the mean of three experiments. Standard deviations are indicated by error bars. Strains were *CDC1* (FY70) and *cdc1-1* (FY11) or derivatives containing the *cos10* (*cos10-28*), *cos2* (*cos2-13*), or *pmc1* (*pmc1*Δ::*LEU2*) allele.

TABLE 1. *PMC1-lacZ* and *PMR2A-lacZ* expression in *cdc1*(Ts) mutants

Genotype	β-Galactosidase activity (U/0.1 OD_{600})[a]			
	PMR2A-lacZ		*PMC1-lacZ*	
	23°C	33°C	23°C	33°C
cdc1-1	29.6 (1.6)	ND	10.2 (1.0)	ND
CDC1	2.0 (0.4)	ND	0.7 (0.1)	ND
cdc1-2	1.2 (0.2)	11.7 (0.8)	0.2 (0.1)	2.9 (0.3)
cdc1-2 [*CDC1*][b]	0.8 (0.2)	1.7 (0.1)	0.2 (0.1)	0.4 (0.1)
*cdc1-2 cnb1*Δ	ND	1.6 (0.3)	ND	0.2 (0.1)
*cdc1-2 cnb1*Δ [*CDC1*][b]	ND	1.6 (0.2)	ND	0.2 (0.1)

[a] Means from at least three independent experiments with two independent transformants. Standard deviations are shown in parentheses. ND, not determined.

[b] Strains with [*CDC1*] carried the *CDC1* plasmid pFB383.

cdc1-1(Ts) mutant. To determine if either Ca^{2+} sensitivity or conditional growth could be explained by an increase in $[Ca^{2+}]_i$, we measured activity of the cytosolic, Ca^{2+}/calmodulin-dependent protein phosphatase, calcineurin. Calcineurin activation by Ca^{2+} results in induction of the genes *PMC1* and *PMR2A*, which encode a vacuolar Ca^{2+}-ATPase and a plasma membrane Na^+/Li^+-ATPase, respectively (6). Expression of *PMC1* and *PMR2A* can be monitored by measuring the β-galactosidase activity of strains containing fusions between these genes and *lacZ*, thereby allowing an indirect readout of in vivo calcineurin activity (6). As shown in Table 1, Cdc1-compromised strains exhibit increases in *PMC1-lacZ* and *PMR2A-lacZ* expression. At 23°C, *cdc1-1*(Ts) strains exhibited β-galactosidase levels 10- to 15-fold higher than those exhibited by isogenic *CDC1* or congenic *cdc1-2*(Ts) strains (Table 1). Thus, Cdc1 diminution results in an increase in expression of two genes under control of the Ca^{2+}-dependent phosphatase, calcineurin. The increase in *PMR2A* expression is consistent with the observation that a *cdc1-1*(Ts) mutant is more resistant to Li^+ than a wild-type *CDC1* strain (data not shown).

To confirm that the increase in *PMC1* and *PMR2A* expression reflected calcineurin activation, we repeated the β-galactosidase assays in strains lacking the calcineurin regulatory subunit, Cnb1. Strains depleted of Cdc1 activity require some calcineurin function (25). Although we do not understand the physiological basis of this requirement, we were unable to construct a double mutant containing the *cdc1-1*(Ts) allele, which is partially inactive at 23°C, and a mutation in calcineurin. The *cdc1-2*(Ts) *PMC1-lacZ* and *cdc1-2*(Ts) *PMR2A-lacZ* strains exhibited growth defects after 6 h at 33°C (data not shown) and displayed β-galactosidase activities that were 7- to 10-fold higher than those observed in the same strains at 23°C (Table 1). Disruption of *CNB1* (*cnb1*Δ::*LEU2*) completely abolished the increases but had little effect on reporter gene expression in the *CDC1* background (Table 1). The low β-galactosidase activity of the *cdc1-2*(Ts) *cnb1*Δ::*LEU2* double mutant was not due to poor growth because *cdc1-2*(Ts) and *cdc1-2*(Ts) *cnb1*Δ::*LEU2* strains containing an unrelated fusion, *JNM1-lacZ*, exhibited similar β-galactosidase activities at 33°C (20.1 and 19.6, respectively). Thus, Cdc1-compromised cells display an increase in calcineurin-dependent transcriptional activity which, in turn, is consistent with an increase in cytosolic Ca^{2+}.

***cos10*/*mid1* mutations suppress the growth and Ca^{2+} hyperaccumulation defects of *cdc1*(Ts) mutants.** The conditional growth defect of *cdc1*(Ts) mutants can be alleviated by Mn^{2+} supplementation (20, 25). Interestingly, Mn^{2+} supplementa-

tion largely restored *cdc1*(Ts) Ca^{2+} accumulation to wild-type levels (Fig. 3). To examine the correlation between the growth and Ca^{2+} accumulation defects further, we determined Ca^{2+} contents of *cdc1-1*(Ts) revertants. Two (*cos10* and *cos2*) of 15 complementation groups identified as recessive suppressors of the *cdc1-1*(Ts) temperature-sensitive growth defect (25) reduced the intracellular Ca^{2+} levels of the *cdc1-1*(Ts) mutant, as well as the wild-type *CDC1* strain (Fig. 3). Thus, the products of both suppressors play a Cdc1-independent role in the maintenance of intracellular Ca^{2+}. Moreover, these results are consistent with the notion that the (*cos10* and *cos2*) suppressors alleviate the *cdc1-1*(Ts) growth defect by inhibiting Ca^{2+} accumulation.

The wild-type *COS10* gene was isolated from a low-copy-number *URA3* library (26) by its ability to complement the recessive *cos10-28* suppressor. Subcloning and physical analyses (data not shown and Materials and Methods) revealed that the minimal complementing region contained a single open reading frame identical to a gene, *MID1*, previously identified in a screen for genes involved in Ca^{2+} influx and mating-pheromone-induced death (15). As expected, a *mid1*Δ::*LEU2* deletion suppressed the *cdc1-1*(Ts) growth defect (see Fig. 5B).

The *COS2*/*CCH1* gene product bears sequence similarity to the α1 subunit of voltage-gated calcium channels. Despite numerous attempts with both low- and high-copy-number yeast libraries, we were unable to clone *COS2* by complementation. The discrepancy in mutation frequency between *cos2* (seven alleles) and *mid1* (one allele, 548 amino acids) suggested that *COS2* might be an unusually large gene and therefore underrepresented in size-selected yeast libraries. Because *cos2* mutations reduced Ca^{2+} levels of both wild-type and *cdc1-1*(Ts) strains, we scanned the yeast sequence database for large proteins that might function in Ca^{2+} uptake. The most prominent of these was an open reading frame (YGR217w) on the right arm of chromosome VII that was predicted to encode a protein of 2,039 amino acids (6,117 bases). Intriguingly, the YGR217w protein bore significant sequence similarity to the α1 subunit of the dihydropyridine-sensitive (L-type) family of voltage-dependent calcium channels (1, 3, 20). (The YGR217w open reading frame is also listed as *CCH1* [for calcium channel homolog] in the *Saccharomyces* Genome Database. YGR217w/*CCH1* has not been described in the literature. However, to avoid possible future confusion, we have adopted the *CCH1* gene name and will hereafter refer to *COS2* as *CCH1*.) Although overall sequence similarity between Cch1 and the α1 subunits is low (24% identity over the lengths of the proteins), several key features such as size, topology, and domain structure of the α1 subunits are retained by Cch1. For example, Cch1 protein, like the α1 subunits, contains four repeat units (I to IV) of six transmembrane domains (Fig. 4A) that tetramerize to form the core of the Ca^{2+} channel (3, 9, 14). Indeed, most of the sequence identity between Cch1 and the mammalian calcium channel subunits is present within regions thought to play key roles in defining channel specificity (domain P) and voltage dependence (transmembrane domain S4). All four hydrophobic domains (I, II, III, and IV) contain amino acid residues indicative of the Ca^{2+}-selective P segment, and three (II, III, and IV) of the four (Fig. 4B, upper panel) contain a highly conserved glutamate residue that is thought to play a critical role in Ca^{2+} coordination (3, 9, 14). Interestingly, each of the S4 segments of domains I, II, and III contain repeated motifs of a positively charged residue followed by two hydrophobic residues (Fig. 4B, lower panel). Similar segments have been shown to act as voltage sensors in ion channels of higher eukaryotes (3, 9, 14). Thus, the *CCH1* open reading frame was predicted to encode a protein with structural properties consistent with a role in Ca^{2+} uptake.

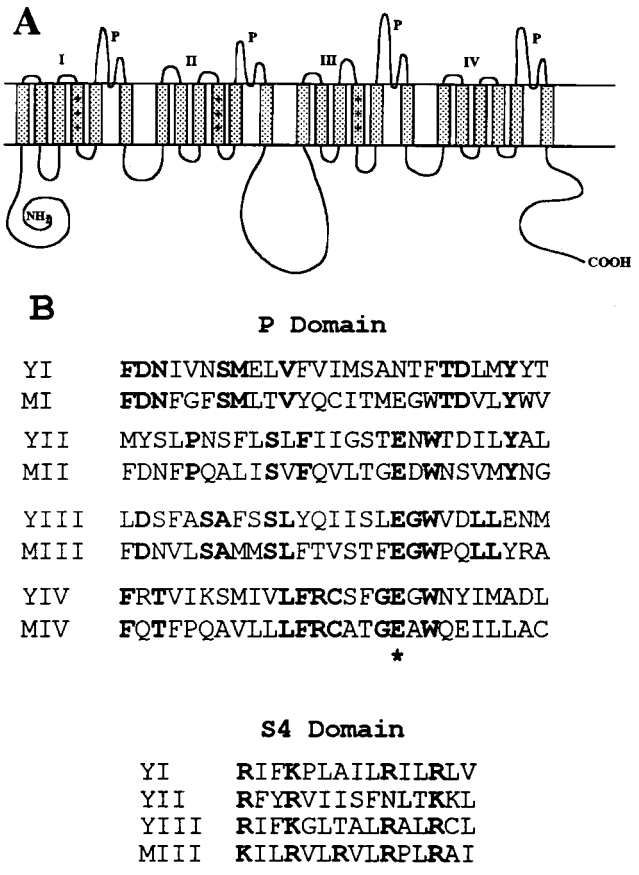

FIG. 4. Characteristics of the Cch1 protein. (A) Schematic diagram of Cch1. The four hydrophobic repeats are marked I to IV. Individual transmembrane domains (excluding the S4 domain of each hydrophobic repeat) were predicted according to the Kyte and Doolittle hydropathy algorithm (18). The S4 and P domains of each hydrophobic repeat were assigned by analogy with mammalian calcium channels. The S4 domains of repeats I, II, and III are marked with plus signs to indicate the positively charged amino acids. (B) Upper panel: sequence alignment of the predicted P domains of Cch1 (YI to YIV) with the corresponding P domains (MI to MIV) of a skeletal muscle Ca^{2+} channel (34). Lower panel: sequence alignment of the positively charged S4 transmembrane segments of Cch1 (YI, YII, and YIII) with the S4 segment of the third hydrophobic repeat (MIII) of a rat brain calcium channel (29).

To determine the identities of *CCH1* and *COS2*, we obtained an internal 2.2-kb fragment of *CCH1* by PCR amplification of yeast chromosomal DNA (see Materials and Methods) and then created a *cch1*Δ::*LEU2* deletion by replacing the internal 1.25-kb *Eco*RV fragment with the 2.2-kb *Hpa*I fragment of *LEU2* (Fig. 5A). After confirming that *CCH1* was not essential, we transformed a *cdc1-1*(Ts) haploid strain to leucine prototrophy and tested growth at several temperatures. As shown in Fig. 5B, the *cdc1-1*(Ts) *cch1*Δ::*LEU2* strain, like the *cdc1-1*(Ts) *mid1*Δ::*LEU2* strain, grew at the nonpermissive temperature [note that *cch1*Δ::*LEU2* and *mid1*Δ::*LEU2* suppressed the *cdc1-1*(Ts) growth defect at 30°C but, like the original spontaneous suppressors, *cos10* and *cos2*, failed to alleviate the growth defect at 36°C.] In addition, diploids formed between the *cdc1-1*(Ts) *cch1*Δ strain and several *cdc1-1*(Ts) *cos2* spontaneous mutants grew at 30°C (data not shown). Because *cch1*Δ and *cos2* mutations were recessive (data not shown), this result suggested that *CCH1* and *COS2* were allelic. Finally, identity was confirmed by genetic linkage,

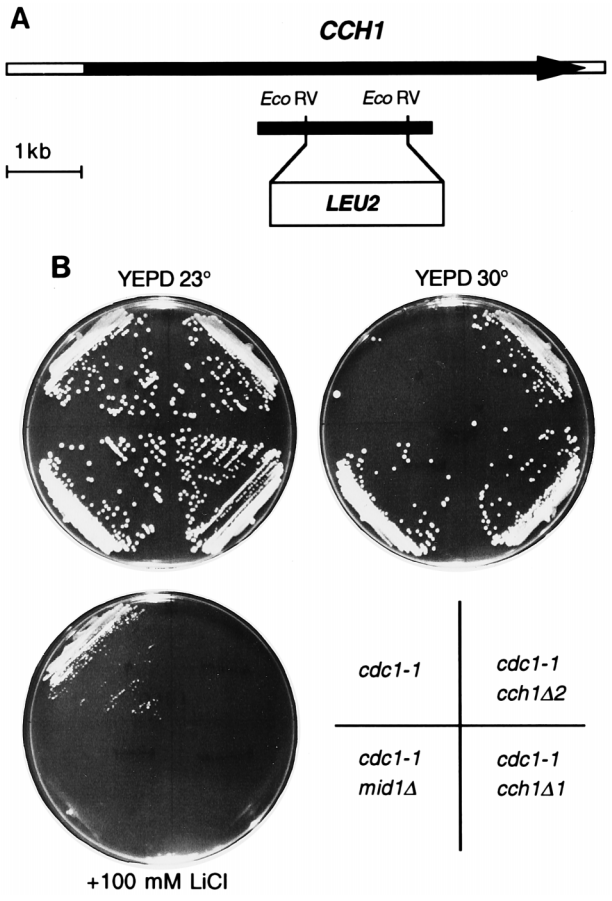

FIG. 5. Characterization of *CCH1* (*COS2*). (A) Schematic of the *CCH1* open reading frame and *cch1*Δ::*LEU2* disruption. The first line shows the complementing PCR fragment and predicted coding region (arrow) of *CCH1*. The second line shows the internal PCR fragment of *CCH1* used to construct the *cch1*Δ::*LEU2* deletion. The *Eco*RV sites used to construct the *cch1*::*LEU2* deletion are shown and are unique to *CCH1*. (B) Suppression of *cdc1-1*(Ts) by disruption of *CCH1* or *MID1*. The indicated strains (*cdc1-1* [*cdc1-1 CCH1 MID1*], *cdc1-1 cch1*Δ*2* [*cdc1-1 cch1-2*Δ::*LEU2 MID1*], *cdc1-1 cch1*Δ*1* [*cdc1-1 cch1-1*Δ::*LEU2 MID1*], and *cdc1-1 mid1*Δ [*cdc1-1 CCH1 mid1*Δ]) were streaked onto YEPD medium or YEPD medium containing 100 mM LiCl and incubated at 23°C (3 days) or 30°C (2 days).

which showed that all *cdc1-1*(Ts) spores from crosses between *cdc1-1*(Ts) *cos2-13* and *CDC1 cch1*Δ::*LEU2* (37 tetrads) or *cdc1-1*(Ts) *cos2-16* and *CDC1 cch1*Δ::*LEU2* (35 tetrads) haploid strains germinated and grew at 30°C.

Interestingly, we have been unable to isolate full-length *CCH1* plasmids in bacteria, even though they can be isolated in yeast and complement the *cch1*Δ::*LEU2* deletion (data not shown). Attempts to recover the full-length clones from yeast into *recA* mutant or *recA*$^+$ bacteria result in gross rearrangements, suggesting that the *CCH1* coding region is deleterious to bacteria. This also could explain why we were unable to clone *CCH1* (*COS2*) from any of the libraries.

***mid1* and *cch1* suppressors block Ca^{2+} accumulation and uptake.** As expected from our studies with the spontaneous suppressors *mid1-28* (*cos10-28*) and *cch1-16* (*cos2-16*), deletion of *MID1* or *CCH1* blocked the increase in intracellular Ca^{2+} elicited by *cdc1-1*(Ts) (Table 2). Moreover, *mid1*Δ and *cch1*Δ mutations reduced intracellular Ca^{2+} contents of *cdc1-1*(Ts) and *CDC1* strains to comparable levels, about 50% of the level exhibited by the wild-type *CDC1 MID1 CCH1* strain (Table 2). Pmc1 inactivation, by contrast, reduced intracellular Ca^{2+} levels of *CDC1* and *cdc1-1*(Ts) strains by similar relative amounts, so that the *cdc1-1*(Ts) *pmc1*Δ double mutant retained twice as much Ca^{2+} as the *CDC1 pmc1*Δ strain (Fig. 3). Thus, Mid1 and Cch1 are necessary for normal Ca^{2+} accumulation and account for Ca^{2+} hyperaccumulation in the *cdc1* (Ts) mutants.

TABLE 2. *cch1* and *mid1* mutations affect Ca^{2+} accumulation in wild-type and *cdc1*(Ts) strains

Genotype	Ca^{2+} accumulation[a] (pmol/OD_{600})	
	CDC1	*cdc1-1*
CCH1 MID1	612.3 (27.2)	1,331.2 (66.2)
*CCH1 mid1*Δ	311.3 (20.4)	319.2 (32.3)
*cch1*Δ *MID1*	294.0 (10.0)	344.7 (28.3)
*cch1*Δ *mid1*Δ	296.6 (16.0)	303.4 (46.4)

[a] Measured by a $^{45}Ca^{2+}$ radiolabeling procedure described previously (5). Values are averages of at least three experiments. Standard deviations are shown in parentheses.

The results shown in Table 2 represent total intracellular Ca^{2+}. However, *mid1*Δ and *cch1*Δ also reduced $[Ca^{2+}]_i$, as measured by the effects of both deletions on *PMR2A* and *PMC1* expression. Table 3 shows that the β-galactosidase levels of *cdc1-1*(Ts) strains containing *PMR2A-lacZ* and *PMC1-lacZ* reporter fusions (6) were elevated, but induction was abrogated by *mid1*Δ and *cch1*Δ deletions. Consistent with this observation, the *cch1*Δ and *mid1*Δ mutations blocked the Li^+ hyperresistance of the *cdc1-1*(Ts) strain (Fig. 5B), presumably by preventing gratuitous expression of *PMR2A*. Finally, *PMR2A* and *PMC1* expression was not affected by either *cch1*Δ or *mid1*Δ under high-Ca^{2+} conditions. Addition of 100 mM Ca^{2+} to *CDC1 cch1*Δ, *CDC1 mid1*Δ, and *CDC1 CCH1 MID1* strains induced reporter gene expression to similar levels (Table 3). Thus, effects of *cch1*Δ and *mid1*Δ are restricted to Ca^{2+}-limiting conditions.

Strains lacking Mid1 function exhibit a defect in basal, as well as pheromone-stimulated, Ca^{2+} uptake activity (15). Accordingly, we examined the role of Cch1 protein in Ca^{2+} accumulation by monitoring $^{45}Ca^{2+}$ uptake in *cch1*Δ, *mid1*Δ, and wild-type strains after α-factor stimulation. As shown in Fig. 6, the *mid1*Δ and *cch1*Δ strains exhibit similar defects in both pheromone-independent and pheromone-activated Ca^{2+} up-

TABLE 3. *cch1* and *mid1* mutations affect gene expression in wild-type and *cdc1*(Ts) strains

Genotype	β-Galactosidase activity (U/0.1 OD_{600})[a]			
	PMR2A-lacZ		PMC1-lacZ	
	—	100 mM	—	100 mM
CDC1				
CCH1 MID1	2.0 (0.4)	275.1 (51.6)	0.7 (0.1)	6.1 (0.8)
*CCH1 mid1*Δ	1.3 (0.1)	178.6 (08.3)	0.2 (0.1)	3.3 (0.8)
*cch1*Δ *MID1*	1.7 (0.6)	277.9 (55.0)	0.3 (0.1)	5.5 (1.2)
cdc1-1				
CCH1 MID1	29.6 (1.6)		10.2 (1.0)	
*CCH1 mid1*Δ	1.4 (0.5)		0.3 (0.1)	
*cch1*Δ *MID1*	1.7 (0.7)		0.3 (0.1)	

[a] Average of at least three experiments with two independent strains. Standard deviations are shown in parentheses. The indicated yeast strains were cultured in normal rich medium (—) or in rich medium containing 100 mM $CaCl_2$ (100 mM).

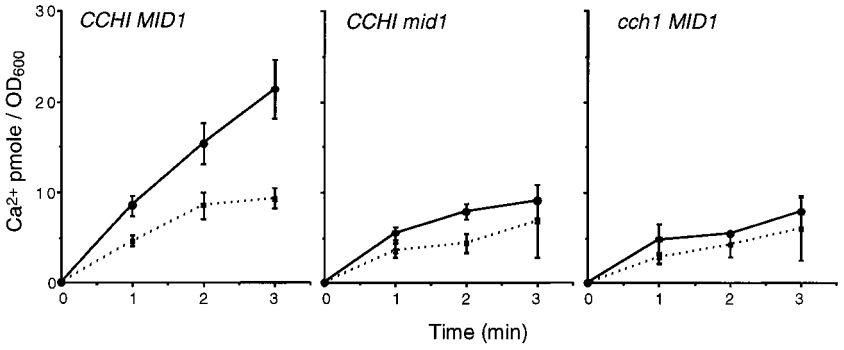

FIG. 6. Ca^{2+} uptake. Pheromone was (solid lines) or was not (dashed lines) added at 6 μM to cultures 45 min prior to addition of $^{45}Ca^{2+}$. Strains were *CCH1 MID1* (*CDC1 CCH1 MID1*), *CCH1 mid1* (*CDC1 CCH1 mid1*Δ), and *cch1 MID1* (*CDC1 cch1*Δ *MID1*).

take compared with the wild-type strain. Together, these results support the hypothesis that mutations in *MID1* and *CCH1* alleviate the *cdc1*(Ts) growth defect by blocking Ca^{2+} uptake and accumulation in the cytosol.

Mutants lacking Cch1 or Mid1 lose viability on pheromone treatment. The isolation of *mid1* lesions in a screen for mutants that die after α-factor treatment is consistent with a role for Mid1 in pheromone-induced Ca^{2+} uptake (15). To determine if Cch1-deficient cells also fail to recover after α-factor-induced arrest, we performed a mating-pheromone halo assay (22). Although all of the strains arrested upon α-factor treatment, only cells of the wild-type strain recovered, as determined by the gradual filling in of the halo surrounding the pheromone disc (Fig. 7). Halos formed on the *mid1*Δ and *cch1*Δ strains did not fill in even after prolonged incubation (Fig. 7). Hence, both Mid1 and Cch1 are required for recovery from α-factor arrest. To determine if the failure to recover reflected a loss of viability, we measured cell viability of pheromone-treated wild-type, *mid1*Δ, *cch1*Δ, and *cnb1*Δ strains. Whereas 3.1% ± 0.9% of the cells of a wild-type culture stained with methylene blue after 12 h of α-factor treatment, 29.5% ± 4.1%, 23.0% ± 1.6%, and 12.5% ± 4.1% of the cells of *cch1*Δ, *mid1*Δ, and *cnb1*Δ cultures, respectively, stained. Finally, stained cells from the *cch1*Δ, *mid1*Δ, and *cnb1*Δ cultures (but not the wild-type strain) displayed a characteristic small-shmoo morphology (15). Thus, *CCH1*-dependent Ca^{2+} uptake is necessary for viability.

Mid1 and Cch1 function in the same Ca^{2+} uptake process. Voltage-gated calcium channels of higher organisms comprise three to four polypeptides. These include the α1 subunit, which contains the calcium-conducting pore, as well as several ancillary subunits (α2δ, β, and γ) that are thought to affect the time course and/or voltage dependence of activation and inactivation (9, 14). Although there are no structural homologs of the ancillary proteins in yeast, the similar characteristics of *cch1* and *mid1* mutants suggested that the products of both genes might be required for pheromone (and *cdc1*)-induced Ca^{2+} uptake. To determine if the two proteins function in the same process, we measured Ca^{2+} levels in strains containing *cch1*Δ and *mid1*Δ deletions alone, as well as in a *cch1*Δ *mid1*Δ double mutant. As shown in Table 2, the double mutant was affected to the same extent as each single mutant, consistent with the hypothesis that Cch1 and Mid1 affect Ca^{2+} uptake by a single mechanism. This conclusion was supported by the similar effects of double and single mutations on *cdc1-1*(Ts) suppression (data not shown).

Mutations in *MID1* and *CCH1* reduced Ca^{2+} uptake and accumulation even under nonstimulating conditions (Fig. 3 and 6; Tables 2 and 3). If Mid1/Cch1-dependent Ca^{2+} uptake served a broader physiological role than recovery from shmoo formation, Ca^{2+} uptake should be affected by *cch1* and *mid1* mutations in a *MAT***a**/*MAT*α diploid strain that can neither mate nor respond to pheromone. In fact, the Ca^{2+} levels of both *CDC1*/*CDC1* (456 ± 37 [*CCH1*/*cch1-16*] and 297 ± 11 [*cch1*Δ/*cch1-16*] pmol/OD_{600}) and *cdc1-1*/*cdc1-1* (1,684 ± 71 [*CCH1*/*cch1-16*] and 252 ± 15 [*cch1*Δ/*cch1-16*] pmol/OD_{600}) diploid strains were affected by the *cch1*Δ::*LEU2* deletion, suggesting these proteins function in Ca^{2+} uptake even under conditions in which mating factor does not elicit a response. Interestingly, Cch1 and Mid1 are also instrumental in the response of a wild-type *CDC1* strain to ion stress, as shown by the Li^{+}-sensitive phenotypes of the *cch1*Δ and *mid1*Δ mutants (Fig. 8). Although calcineurin has been implicated in the ion stress response (21, 23), this finding provides the first direct evidence that the signal is generated, or at least maintained, by external Ca^{2+}. Finally, *cch1*Δ and *mid1*Δ single mutants were as sensitive to Li^{+} as the *cch1*Δ *mid1*Δ double mutant (Fig. 8), providing further support for the hypothesis that Mid1 and Cch1 function in the same Ca^{2+} uptake process.

DISCUSSION

The *cdc1*(Ts) growth defect is exacerbated by high intracellular calcium. Previous reports linked the *cdc1*(Ts) growth defect to depletion of an intracellular Mn^{2+}-dependent function (20, 25, 32). One study also suggested that the conditional growth defect could be weakly ameliorated by addition of high levels (100 mM) of exogenous Ca^{2+} (20). Based on those results, Loukin and Kung (20) hypothesized that Mn^{2+} and Ca^{2+} might be interchangeably required for an essential, Cdc1-dependent function. Consistent with that hypothesis, Mn^{2+}

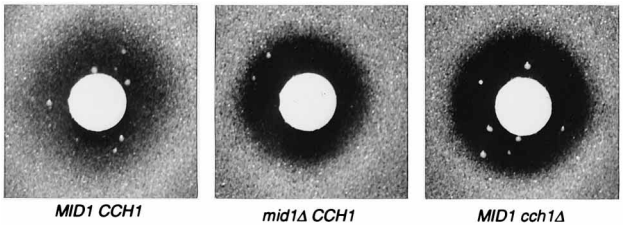

FIG. 7. *cch1* mutations confer a Mid^{-} phenotype. Cultures of the indicated strains (*MID1 CCH1* [*CDC1 MID1 CCH1*], *mid1*Δ *CCH1* [*CDC1 mid1*Δ *CCH1*], and *MID1 cch1*Δ [*CDC1 MID1 cch1*Δ]) were transferred to solid rich medium in top agar, where they were incubated at 30°C for 4 days in the presence of filters impregnated with 4 nmol of α-factor.

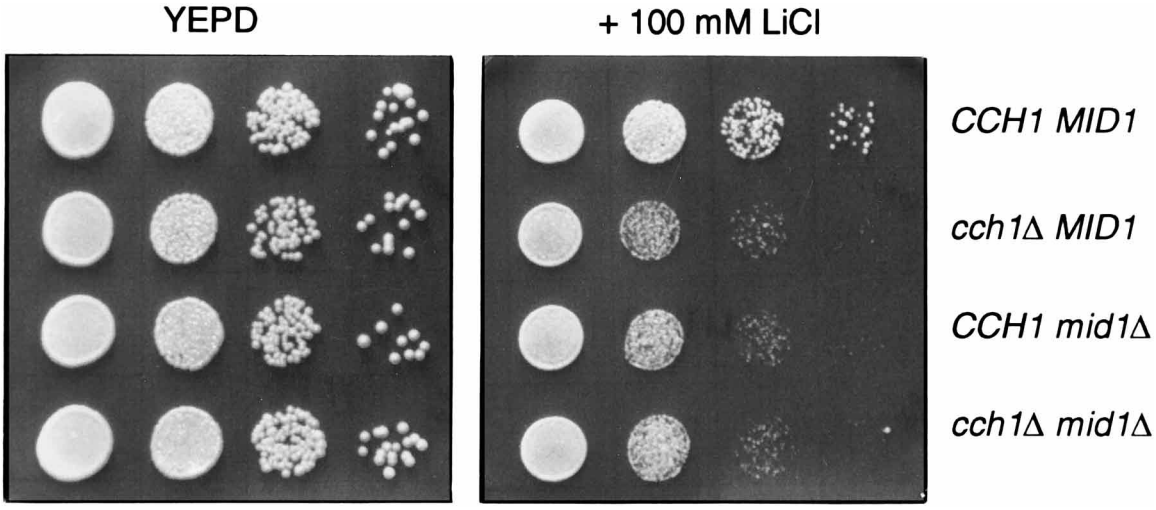

FIG. 8. Li^+ sensitivity of *mid1*Δ and *cch1*Δ mutants. Tenfold serial dilutions of log-phase cultures were spotted onto rich medium agar without (YEPD) or with 100 mM LiCl. Strains were *CCH1 MID1* (*CDC1 CCH1 MID1*), *cch1*Δ *MID1* (*CDC1 cch1*Δ *MID1*), *CCH1 mid1*Δ (*CDC1 CCH1 mid1*Δ), and *cch1*Δ *mid1*Δ (*CDC1 cch1*Δ *mid1*Δ).

supplementation is capable of restoring growth to a *cdc1*Δ deletion strain (25). However, the studies described here show that *cdc1*(Ts) mutants are sensitive to high-Ca^{2+} (200 mM) conditions (Fig. 1). Although the reason for the discrepancy is not known, the residual growth elicited by high external Ca^{2+} at the nonpermissive temperature (20) could reflect osmotic protection (25) rather than Ca^{2+} remediation.

Of the Ca^{2+}-sensitive yeast mutants characterized to date, several accumulate excess intracellular Ca^{2+} under normal growth conditions (1, 24, 33). These mutants are thought, or have been shown, to contain defects in ion homeostasis which result in the buildup of toxic levels of intracellular Ca^{2+} during growth in Ca^{2+}-rich medium. Interestingly, Ca^{2+} accumulation also accounts for the *cdc1*(Ts) temperature-sensitive growth defect. *cdc1*(Ts) strains accumulate excess intracellular Ca^{2+} under low-Ca^{2+} conditions (Fig. 2 and Table 2), and the extent of accumulation is directly related to the severity of the growth defect. Although this finding provides only circumstantial support for a causal relationship between Ca^{2+} accumulation and conditional growth, mutations that block Ca^{2+} uptake (Fig. 3 and 6; Table 2) also suppress the *cdc1*(Ts) temperature-sensitive growth defect (Fig. 5B). These mutations inactivate genes (*MID1* and *CCH1*) that are necessary for high-affinity Ca^{2+} uptake and accumulation (see below); hence it seems likely that suppression is a direct consequence of their effect on intracellular Ca^{2+} levels.

In contrast to other genes identified in Ca^{2+}-sensitive screens, *CDC1* is essential even in medium containing low external Ca^{2+} (Fig. 5B). This difference could reflect the fact that Cdc1 depletion results in the activation of a high-affinity Ca^{2+} uptake system (Fig. 2), whereas the other genes are primarily involved in ion sequestration (1, 24, 33). In this scenario, Ca^{2+} toxicity alone could account for the conditional growth defect of the *cdc1*(Ts) mutants. An alternative explanation is that Ca^{2+} accumulation, stimulated by Cdc1 depletion (see below) or growth in high-Ca^{2+} conditions, exacerbates the loss of an essential, Cdc1-dependent function. Consistent with the latter interpretation, neither *mid1*Δ nor *cch1*Δ is capable of suppressing the *cdc1*(Ts) growth defect at 36°C (Fig. 5B; reference 25). The simplest interpretation of this result is that Cdc1 depletion results in a biochemical defect that is exacerbated by Ca^{2+} accumulation.

How does Ca^{2+} accumulation exacerbate the *cdc1*(Ts) growth defect? Our results do not directly address the biochemical nature of the Ca^{2+} toxicity; however, we favor a model in which the *cdc1*(Ts) Mn^{2+} homeostasis defect (25) is aggravated by activation of the cytosolic, Ca^{2+}-dependent phosphatase, calcineurin. Vacuolar Ca^{2+} does not account for the effects of Ca^{2+} because *cdc1*(Ts) temperature-sensitive growth is unaffected by a mutation (*pmc1*Δ) that prevents Ca^{2+} from accumulating in the vacuole. By contrast, *cdc1*(Ts) Ca^{2+} toxicity correlates well with $[Ca^{2+}]_i$ and calcineurin activity. For example, cytosolic Ca^{2+} pools are elevated in the *cdc1*(Ts) mutant (Fig. 3 and Table 1), and *cdc1*(Ts) Ca^{2+} sensitivity is exacerbated (Fig. 1) by a mutation (*pmc1*Δ) that blocks Ca^{2+} efflux from the cytosol (6). In addition, calcineurin activity is elevated in *cdc1*(Ts) strains exhibiting a growth defect (Fig. 5B and Table 1). Calcineurin activation stimulates the expression of a number of yeast ion homeostasis genes (4, 6, 21, 23), including the Mn^{2+} transporter gene, *PMR1* (6). *PMR1* encodes a Ca^{2+}/Mn^{2+} pump of the Golgi that delivers manganese ions from the cytosol to the secretory pathway (19). Thus, enhanced *PMR1* expression might aggravate the *cdc1*(Ts) Mn^{2+} defect by stimulating Mn^{2+} efflux from the cell. Consistent with this scenario, *PMR1* overexpression severely compromises *cdc1-1*(Ts) growth (25). Although this finding does not prove that *PMR1* is responsible for *cdc1*(Ts) Ca^{2+} toxicity, it provides a simple mechanism for how Ca^{2+}, through calcineurin, might exacerbate an intracellular Mn^{2+} defect. Alternatively, calcineurin could aggravate the *cdc1*(Ts) Mn^{2+} defect by its documented role in restricting Mn^{2+} uptake (12).

Ca^{2+} channels in yeast. Several observations support the assertion that Cch1 is an essential component of a high-affinity calcium channel. First, strains lacking Cch1 exhibit a biochemical defect in Ca^{2+} uptake and accumulation in low-Ca^{2+} medium. For example, the *cch1*Δ mutation caused a reduction in total and cytosolic Ca^{2+} accumulation (Tables 2 and 3), presumably by impairing basal, as well as pheromone-stimulated, Ca^{2+} influx (Fig. 6; reference 15). Second, *cch1*Δ strains exhibit a phenotype (Fig. 7) characteristic of strains unable to

mount, or respond to, a pheromone-induced Ca^{2+} increase (15). Third, *cch1*Δ mutants exhibit a defect in a calcineurin-dependent ion stress response (Fig. 8). Although it has been generally assumed that cytosolic Ca^{2+} mediates the ion stress response (21, 23), this result provides the first evidence that Ca^{2+} uptake is important for adaptation to high salt. Finally, *cch1* and *mid1* mutations were isolated as recessive suppressors of *cdc1-1*(Ts) temperature-sensitive growth, a defect that is associated with elevated intracellular Ca^{2+} (Fig. 2 and 3; Tables 1 and 2). The *MID1* gene encodes a plasma membrane protein involved in pheromone-stimulated Ca^{2+} uptake. Although we have not localized Cch1 protein, the similar phenotypes and biochemical defects of strains lacking Cch1, Mid1, or both Cch1 and Mid1 suggest that these two proteins form a channel necessary for Ca^{2+} influx across the plasma membrane.

A second line of evidence to support the hypothesis that Cch1 is an essential component of a Ca^{2+} channel is the sequence similarity between Cch1 and the α1 subunits of L-type, voltage-gated calcium channels. Although the overall sequence similarity is limited (24% over the entire length of the protein), the size and predicted structures and topologies are conserved between Cch1 and its mammalian counterparts (3, 9, 14). Moreover, sequence similarity is most apparent in the four hydrophobic domains that are believed to tetramerize and form the channel pore (9, 14). Finally, two subdomains of the hydrophobic repeats of mammalian α1 subunits are well conserved in Cch1 (Fig. 4B). Three of the four predicted hydrophobic domains of Cch1 contain a stretch of repeating triplets of arginine (or lysine) residues followed by two hydrophobic amino acids. Similar regions form alpha-helical transmembrane (S4) domains in the four repeats of the mammalian proteins and may confer voltage dependence upon the channels. Although the functional importance of these domains to Cch1 function remains to be tested, the amino acid and topological conservation of this positively charged region within Cch1 is striking. A second characteristic of calcium-specific, voltage-dependent channels is the presence of so-called P segments within each of the four hydrophobic domains. Conserved glutamate residues within each P domain determine ion selectivity by coordinating Ca^{2+}. Three of the four P segments of the yeast Cch1 protein also contain a conserved glutamate residue, and the fourth domain contains a small polar residue (asparagine).

Identification of a putative voltage-dependent calcium channel in yeast, a genetically tractable organism, provides the opportunity to address questions that are difficult or impossible to address in higher eukaryotes. Of particular interest are the mechanisms by which Ca^{2+} channels are regulated. Recent results have suggested that mammalian Ca^{2+} channels can be inhibited through direct interaction with the βγ subunits of receptor-activated trimeric G proteins (10). It is thus intriguing that a free βγ complex (products of the *STE4* and *STE18* genes, respectively) activates the pheromone response pathway in yeast (30). However, it seems unlikely that the Mid1/Cch1 channel is directly regulated by the βγ subunit, since pheromone-stimulated Ca^{2+} uptake requires the downstream transcriptional activator, Ste12 (25), as well as protein synthesis (15). Mammalian Ca^{2+} channels are also thought to be activated by depletion of internal Ca^{2+} stores (31). *cdc1*(Ts) mutations result in localized Mn^{2+} depletion (20, 25, 32), and so it is tempting to speculate that the yeast Ca^{2+} channel might also be regulated by intracellular Mn^{2+} levels. Consistent with this hypothesis, Mn^{2+} supplementation restored Ca^{2+} channel activity of the *cdc1*(Ts) mutant to the basal level of a wild-type strain (Fig. 3). Unfortunately, the sequence of the Cdc1 protein (20) has not suggested an obvious mechanism for this regulation.

An equally important question concerns the physiological importance of the Mid1/Cch1 Ca^{2+} channel. It is clear from our results (Fig. 7), as well as the results of others (15), that both Cch1 and Mid1 are necessary for Ca^{2+}-dependent viability during pheromone-mediated arrest (7, 8, 22). However, Cch1 and Mid1 are also activated by Cdc1 depletion (Fig. 3), are essential for full response to ion stress (Fig. 8), and are functional in a strain that is unable to respond to pheromone addition (Table 3). Thus, the Cch1/Mid1 Ca^{2+} channel may play important, albeit unknown, roles in processes unrelated to mating. Identification of Cch1 as the first microbial member of a large class of Ca^{2+} channels should allow this and other questions to be answered.

ACKNOWLEDGMENTS

We thank K. Cunningham and C. Hemmenway for generously providing plasmids, C. Alarcon for donating genomic DNA, and J. Heitman, D. Lew, and A. Means for helpful comments on the manuscript.

M. Paidhungat was supported in part by the Cell and Molecular Biology Training Program of Duke University.

REFERENCES

1. **Beeler, T., K. Gable, C. Zhao, and T. Dunn.** 1994. A novel protein, CSG2p, is required for Ca^{2+} regulation in *Saccharomyces cerevisiae*. J. Biol. Chem. **10:**7279–7284.
2. **Casadaban, M. J., A. Martinez-Arias, S. K. Shapiro, and J. Chou.** 1983. β-Galactosidase gene fusions for analyzing gene expression in *Escherichia coli* and yeast. Methods Enzymol. **100:**293–308.
3. **Catterall, W. A.** 1995. Structure and function of voltage-gated ion channels. Annu. Rev. Biochem. **64:**493–531.
4. **Cunningham, K., and G. Fink.** 1994. Ca^{2+} transport in *Saccharomyces cerevisiae*. J. Exp. Biol. **196:**157–166.
5. **Cunningham, K., and G. Fink.** 1994. Calcineurin-dependent growth control in *Saccharomyces cerevisiae* mutants lacking *PMC1*, a homolog of plasma membrane Ca^{2+} ATPases. J. Cell Biol. **124:**351–363.
6. **Cunningham, K., and G. Fink.** 1996. Calcineurin inhibits *VCX1*-dependent H^+/Ca^{2+} exchange and induces Ca^{2+} ATPases in *Saccharomyces cerevisiae*. Mol. Cell. Biol. **16:**2226–2237.
7. **Cyert, M. S., and J. Thorner.** 1992. Regulatory subunit (*CNB1* gene product) of yeast Ca^{2+}/calmodulin-dependent phosphoprotein phosphatases is required for adaptation to pheromone. Mol. Cell. Biol. **12:**3460–3469.
8. **Davis, T. N.** 1995. Calcium in *Saccharomyces cerevisiae*. Adv. Second Messenger Phosphoprotein Res. **30:**339–358.
9. **De Waard, M., C. A. Gurnett, and K. P. Campbell.** 1996. Structural and functional diversity of voltage-activated calcium channels. Ion Channels **4:** 41–87.
10. **De Waard, M., H. Liu, D. Walker, V. E. S. Scott, C. A. Gurnett, and K. P. Campbell.** 1997. Direct binding of G-protein βγ complex to voltage-dependent calcium channels. Nature **385:**446–450.
11. **Dunn, T., K. Gable, and T. Beeler.** 1994. Regulation of cellular Ca^{2+} by yeast vacuoles. J. Biol. Chem. **269:**7273–7278.
12. **Farcasanu, I. C., D. Hirata, E. Tsuchiya, F. Nishiyama, and T. Miyakawa.** 1995. Protein phosphatase 2B of *Saccharomyces cerevisiae* is required for tolerance to manganese, in blocking the entry of ions into the cells. Eur. J. Biochem. **232:**712–717.
13. **Gaber, R.** 1992. Molecular genetics of yeast ion transport. Int. Rev. Cytol. **137A:**299–353.
14. **Hofmann, F., M. Biel, and V. Flockerzi.** 1994. Molecular basis for Ca^{2+} channel diversity. Annu. Rev. Neurosci. **17:**399–418.
15. **Iida, H., H. Nakamura, T. Ono, M. S. Okumura, and Y. Anraku.** 1994. *MID1*, a novel *Saccharomyces cerevisiae* gene encoding a plasma membrane protein, is required for Ca^{2+} influx and mating. Mol. Cell. Biol. **14:**8259–8271.
16. **Iida, H., Y. Yagawa, and Y. Anraku.** 1990. Essential role for induced Ca^{2+} influx followed by $[Ca^{2+}]_i$ rise in maintaining viability of yeast cells late in the mating pheromone response pathway. J. Biol. Chem. **265:**13391–13399.
17. **Kaiser, C., S. Michaelis, and A. Mitchell.** 1994. Methods in yeast genetics. Cold Spring Harbor Laboratory Press, Plainview, N.Y.
18. **Kyte, J., and R. F. Doolittle.** 1982. A simple method for displaying the hydropathic character of a protein. J. Mol. Biol. **157:**105–132.
19. **Lapinskas, P. J., S. Lin, and V. C. Culotta.** 1996. The role of the *Saccharomyces cerevisiae CCC1* gene in the homeostasis of manganese ions. Mol. Microbiol. **21:**519–528.
20. **Loukin, S., and C. Kung.** 1995. Manganese effectively supports yeast cell-cycle progression in place of calcium. J. Cell Biol. **131:**1025–1037.

21. **Mendoza, I., F. Rubio, A. Rodriguez-Navarro, and J. M. Pardo.** 1994. The protein phosphatase calcineurin is essential for NaCl tolerance of *Saccharomyces cerevisiae*. J. Biol. Chem. **269:**8792–8796.
22. **Moser, M. J., J. R. Geiser, and T. N. Davis.** 1996. Ca^{2+}-calmodulin promotes survival of pheromone-induced growth arrest by activation of calcineurin and Ca^{2+}-calmodulin-dependent protein kinase. Mol. Cell. Biol. **16:**4824–4831.
23. **Nakamura, T., Y. Liu, D. Hirata, H. Namba, S. Harada, T. Hirokawa, and T. Miyakawa.** 1993. Protein phosphatase type 2B (calcineurin)-mediated, FK506-sensitive regulation of intracellular ions in yeast is an important determinant for adaptation to high salt stress conditions. EMBO J. **12:**4063–4071.
24. **Ohya, Y., N. Umemoto, I. Tanida, A. Ohta, H. Iida, and Y. Anraku.** 1991. Calcium-sensitive *cls* mutants of *Saccharomyces cerevisiae* showing a pet^- phenotype are ascribable to defects of vacuolar membrane H^+/ATPase activity. J. Biol. Chem. **266:**13791–13977.
25. **Paidhungat, M., and S. Garrett.** Unpublished data.
26. **Rose, M. D., P. Novick, J. H. Thomas, D. Botstein, and G. Fink.** 1987. A *Saccharomyces cerevisiae* genomic plasmid bank based on a centromere-containing shuttle vector. Gene **60:**237–243.
27. **Saimi, Y., B. Martinac, R. R. Preston, X. Zhou, S. Sukharev, P. Blount, and C. Kung.** 1994. Ion channels of microbes. Soc. Gen. Physiol. Ser. **49:**179–185.
28. **Sikorski, R. S., and P. Hieter.** 1989. A system of shuttle vectors and yeast host strains designed for efficient manipulation of DNA in *Saccharomyces cerevisiae*. Genetics **122:**19–27.
29. **Snutch, T. P., W. J. Tomlinson, J. P. Leonard, and M. M. Gilbert.** 1991. Distinct calcium channels are generated by alternative splicing and are differentially expressed in the mammalian CNS. Neuron **7:**45–57.
30. **Sprague, G. F., and J. W. Thorner.** 1992. Pheromone response and signal-transduction during the mating process of *Saccharomyces cerevisiae*, p. 657–744. *In* E. W. Jones, J. R. Pringle, and J. R. Broach (ed.), The molecular and cellular biology of the yeast *Saccharomyces*. Gene expression. Cold Spring Harbor Laboratory Press, Plainview, N.Y.
31. **Striggow, F., and B. E. Ehrlich.** 1996. Ligand-gated calcium channels inside and out. Curr. Opin. Cell Biol. **8:**490–495.
32. **Supek, F., L. Supekova, H. Nelson, and N. Nelson.** 1996. A yeast manganese transporter related to the macrophage protein involved in conferring resistance to mycobacteria. Proc. Natl. Acad. Sci. USA **93:**5105–5110.
33. **Takita, Y., Y. Ohya, and Y. Anraku.** 1995. The *CLS2* gene encodes a protein with multiple membrane-spanning domains that is important for Ca^{2+} tolerance in yeast. Mol. Gen. Genet. **246:**269–281.
34. **Tanabe, T., H. Takeshima, A. Mikami, V. Flockerzi, H. Takahashi, K. Kangawa, M. Kojima, H. Matsuo, T. Hirose, and S. Numa.** 1987. Primary structure of the receptor for the calcium channel blockers from skeletal muscle. Nature **328:**313–318.
35. **Withee, J. L., J. Mulholland, R. Jeng, and M. S. Cyert.** 1997. An essential role of the yeast pheromone-induced Ca^{2+} signal is to activate calcineurin. Mol. Biol. Cell. **8:**263–267.
36. **Woodcock, D. M., P. J. Crowther, J. Doherty, S. Jefferson, E. DeCruz, M. Noyer-Weidner, S. S. Smith, M. Z. Michael, and M. W. Graham.** 1989. Quantitative evaluation of *Escherichia coli* host strains for tolerance to cytosine methylation in plasmid and phage recombinants. Nucleic Acids Res. **17:**3469–3478.
37. **Youatt, J.** 1993. Calcium and microorganisms. Crit. Rev. Microbiol. **19:**83–97.